Steel and Composite Structures, Vol. 1, No. 4 (2001) 393-410
DOI: http://dx.doi.org/10.12989/scs.2001.1.4.393

Structural behavior of slender circular steel-concrete composite columns under various means of load application

Mathias Johansson† and Kent Gylltoft‡

Department of Structural Engineering, Concrete Structures, Chalmers University of Technology, SE-412 96 Göteborg, Sweden

Abstract. In an experimental and analytical study on the structural behavior of slender circular steel-concrete composite columns, eleven specimens were tested to investigate the effects of three ways to apply a load to a column. The load was applied eccentrically to the concrete section, to the steel section or to the entire section. Three-dimensional nonlinear finite element models were established and verified with the experimental results. The analytical models were also used to study how the behavior of the column was influenced by the bond strength between the steel tube and the concrete core and the by confinement of the concrete core offered by the steel tube. The results obtained from the tests and the finite element analyses showed that the behavior of the column was greatly influenced by the method used to apply a load to the column section. When relying on just the natural bond, full composite action was achieved only when the load was applied to the entire section of the column. Furthermore, because of the slenderness effects the columns did not exhibit the beneficial effects of composite behavior in terms of increased concrete strength due to the confinement.

Key words: composite column; confined concrete; bond; load application; hollow steel section; non-linear finite element analyses; experiments.

1. Introduction

Composite columns consisting of concrete-filled steel tubes (CFT) have become increasingly popular in structural applications around the world, often used in moment-resisting frames. This is partly due to their excellent earthquake-resistant properties such as high strength, high ductility, and large energy absorption capacity. Although the risk of a major earthquake in Sweden is small, this type of column can offer many other advantages, for instance the increased speed of construction; positive safety aspects; and possible use of simple standardized connections. Furthermore, the steel tube encloses the concrete core and is used as both longitudinal and lateral reinforcement as well as formwork during casting of the concrete. In Sweden, moment-resisting frames are seldom used in multistory buildings; instead they are almost exclusively braced horizontally by shear walls. High frames require large sections of beams and columns and also moment-rigid connections. Such building system tends to be more expensive than braced frames. In principle, two different beam-column systems are used in Sweden; continues columns over 2-3 stories with simple supported beams; and story high columns with continues beams. While most research are concerning seismic issues, the current work is part of an

†Lic. Sc.
‡Professor and Head of Department

ongoing research program to increase the knowledge of the mechanical behavior of CFT columns that will lead to more efficient use of CFT columns in this type of braced structures.

In order to ensure the composite action in the CFT columns, stress transfer is required. In practice this is attained by relying on either the natural bond between the steel and the concrete or mechanical shear connectors on the inside of the tubes; see Roeder *et al*. (1999). However, in CFT columns with smaller dimensions it is of great practical and economic interest not to have any mechanical shear connectors at the interface between the concrete core and the steel tube, and in the absence of shear connectors the composite action has to be achieved by the natural bond. It is believed that the bond strength has a significant effect on the behavior of composite members and Roeder *et al*. (1999) concluded that braced frames had higher bond stress demand than moment resisting frames, especially in regions of geometric discontinuity such as connections where vertical forces are introduced to the column. But careful examination of numerous test results indicates that there is still uncertainty about the effect of bond strength on the structural behavior of slender CFT columns, and this subject has been identified for further research by Shams and Saadeghvaziri (1997).

The purpose of this study was to examine the non-linear response of slender CFT columns with circular section subjected to eccentric loading. The primary focus was on the demand of bond stress to ensure composite action when the loads are applied differently to the top section of the column. To study this, a combination of experiments and nonlinear finite element (FE) analyses was used.

While there have been some experimental studies of slender CFT columns, (Grauers 1993, Kilpatrick and Rangan 1999a, Kilpatrick and Rangan 1999b), there have been less analytical work where the slip and stress transfer between the steel tube and the concrete core concrete has been taken into account. Hajjar *et al.* (1998) presented a fiber based distributed plasticity FE approach for analysis of square and rectangular CFT columns. This model accounts for slip between the concrete and the steel by incorporation of a nonlinear slip interface. Although this model shows good correspondence with experimental results, its advantages are especially in frame analyses where CFT columns are parts of a complete structure. To study the CFT columns more thoroughly, a three-dimensional nonlinear FE model is presented in this paper. The model is based on solid elements with the interfaces between the steel tube and the concrete core simulated with a surface-based interaction using a Coulomb friction model. The surfaces of the concrete and the steel are able to separate and slide relative to each other, as well as transmit contact pressure and shear stresses. Furthermore, both material and geometric nonlinear behavior is taken into account, i.e., confinement effects, local buckling and second-order effects are taken into consideration. These are matters of vital importance if the real stress situation in the column is aimed to study, especially in regions around connection detailing. The first section of this paper describes the experimental part of this study including test set-up, material properties and results. The second gives a detailed description of the established FE model along with the calibration of the model against the experimental results. Next, the results obtained both from the experiments and FE analyses are discussed. Finally, some conclusions are drawn. More information about this study can be found in Johansson (2000).

2. Experiments

2.1. The test program

An experimental study was made on 11 slender columns; see Table 1. The column lengths, l_c, were 2500 mm and the cross-sections were circular with a 159 mm outer diameter. The thickness of the steel

Table 1 Test program for steel-concrete composite columns

Column type[1)]	Filled with concrete	Load application	Buckling length l (mm)	Number of tests
LES	no	steel	2696	2
LFE	yes	entire	2696	3
LFC	yes	concrete	2716	3
LFS	yes	steel	2696	3

[1)]XYZ X = L indicates that it is a Long slender column.
Y = F or E. Indicates if the steel tube is Filled with concrete or Empty.
Z = E, C or S. Indicates if the load is applied to the Entire section, the Concrete section or the Steel section

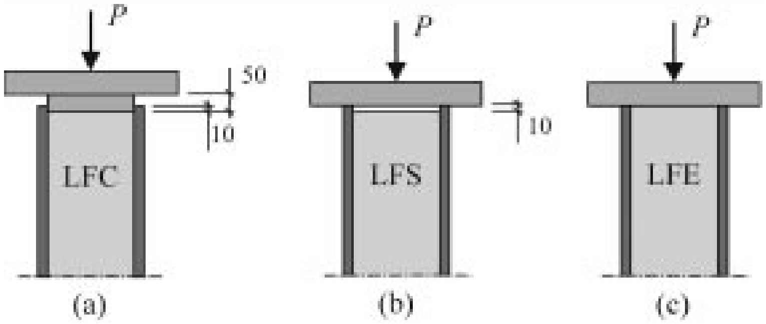

Fig. 1 Three types of load application. Load applied to: (a) the concrete section, (b) the steel section, and (c) the entire section

tubes was 4.8 mm. Nine columns were circular hollow steel sections filled with concrete, while two columns, which were to be used as reference columns, were tested unfilled. The columns were tested to failure under eccentric loading with the axial load applied with an initial end eccentricity of e_{0i} = 10 mm. The parameters varied in the study were the three means of load application. The load was applied to the concrete section (a), to the steel section (b) or to the entire section (c); see Fig. 1. The columns always rested on the entire section at the bottom, and the load application was varied only at the top. In this way a more realistic loading situation was assumed to be achieved. To facilitate load arrangements (a) and (b), the last 10 mm of the columns were left unfilled. The column length is the length of the column itself excluding arrangement for load application. The buckling length, l, is the total length between the loading plates, bearings included. Therefore, the buckling length for the columns loaded at the concrete core had a higher value. All of the tests were carried out in the laboratory of the Department of Structural Engineering, Chalmers University of Technology.

2.2. Materials

The columns were manufactured in the laboratory of the Department of Structural Engineering and the concrete was produced by a local manufacturer. All specimens were cast in a vertical position on the same occasion and with concrete from the same batch. The mean values of the concrete material properties at the age of 28 days are summarized in Table 2. The compressive cylinder strength, $f_{c,cyl}$, and the modulus of elasticity, E_0 and E_c, refer to tests on cylinders (Ø150 × 300 mm). The compressive

Table 2 Material properties of the concrete

$f_{c,cube}$ (MPa)	$f_{c,cyl}$ (MPa)	E_0 (GPa)	E_c (GPa)	G_F (N/m)
79.4	64.5	39.5	38.5	157

Table 3 Material properties of the steel

f_y (MPa)	f_u (MPa)	ε_{ah} (‰)	ε_{au} (‰)	E_a (GPa)
433	568	29	136	206

cube strength, $f_{c,cube}$, refers to tests on cubes ($150 \times 150 \times 150$ mm). The tests of the material properties followed the Swedish Standard, BST Byggstandardisering (1991). The fracture energy, G_F, was determined according to the recommendations of RILEM (1985).

Tensile test specimens of geometry in accordance with the Swedish Standard, SS 11 21 19, were taken out of the steel tubes. The yield strength f_y, the ultimate strength f_u, the strain at hardening ε_{ah}, the ultimate strain ε_{au} and modulus of elasticity E_a of the steel are given in Table 3. The material values given are the average values of five tensile tests.

2.3. Test setup

All of the tests were carried out in a Losenhausen vertical hydraulic column-testing machine with a capacity of 10,000 kN. The columns were hinged at both ends and loaded with a compressive axial load applied with an initial end eccentricity. The eccentricity was equal at both ends and the column was loaded uniaxially. Curved bearing plates of steel, which were fixed to a thick steel plate in contact with the column end, obtained the hinges. The steel plate was provided with another steel plate, in which a hole was drilled, big enough to just fit the column. This procedure was carried out to ensure the correct position of the column in the test rig. The horizontal deflection in the bending direction was measured at column mid-height and also at four additional levels to capture the deformed shape of the column. The vertical displacement of the lower, movable loading plate of the column-testing machine was measured in relation to the laboratory floor. This measured value was assumed to correspond with the vertical displacement of the test specimen. The load arrangement and instrumentation can be seen in Fig. 2. Except for the empty reference columns, strains were measured at 6 points on the outside of the steel tube at mid-height of the columns; see Fig. 3.

The load was evaluated by measurements from an oil pressure gage and was increased manually at a constant rate up to maximum load. The oil pressure gage was then used to indicate how the deformation should be increased to capture the post-peak curve. The displacements were measured by inductive displacement transducers. With the manually controlled deformation, it was possible to study the post-peak behavior of the tests. Thus, it was also possible to study the elastic behavior, the maximum load resistance and the ductility of the columns.

2.4. Test results

The typical structural behaviors of the tested slender columns are represented in Fig. 4 by relations between the load, P, and the horizontal deflection, δ_h, at column mid-height. The horizontal deflection

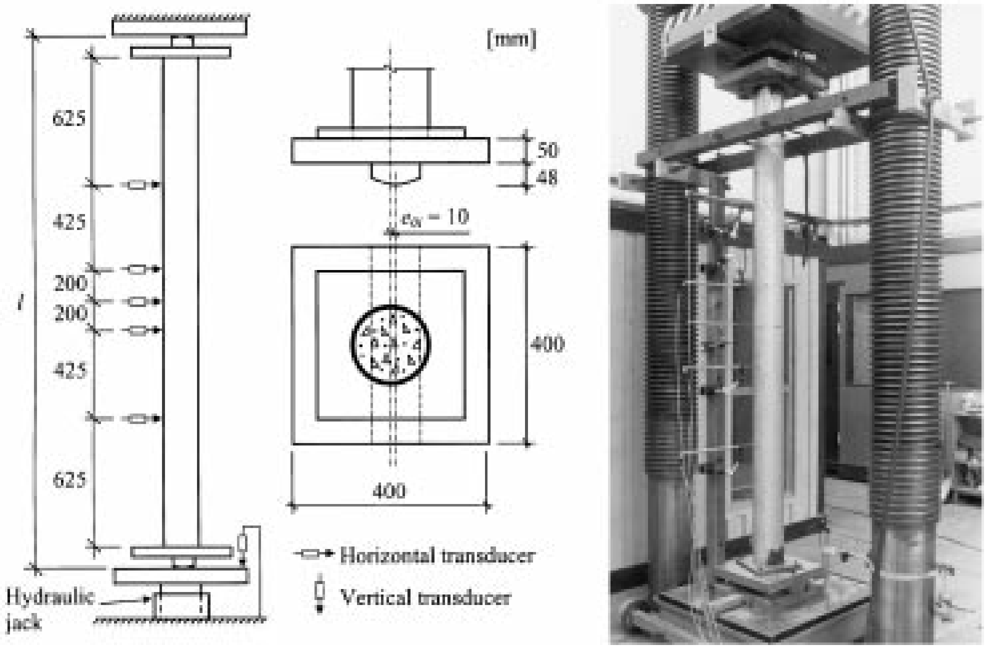

Fig. 2 The principal load arrangement and instrumentation of the columns

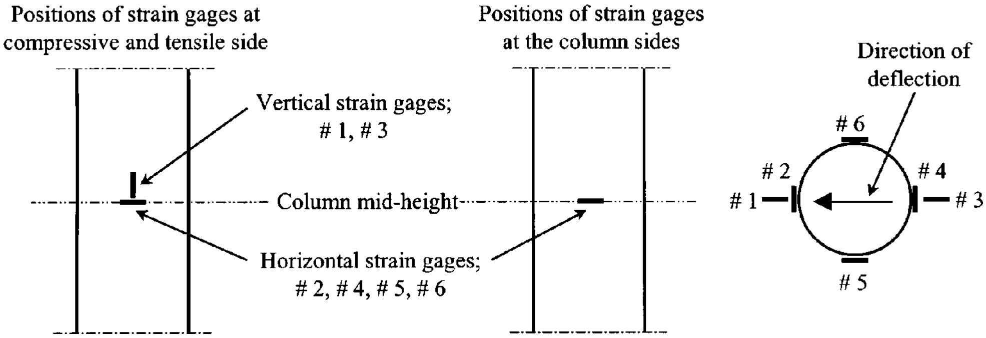

Fig. 3 Positions of the strain gages at mid-height of the columns

presented is the measured one without any correction for the rotation of the support. The initial end eccentricity was 10 mm for all columns. The columns behaved in a stiff manner and the deflection was small during the first part of the loading. Near the maximum load the deflection increased, and after the maximum load was reached, a smoothly falling branch of the load-deflection curve was obtained. For all the composite columns the maximum load resistance was determined by global buckling with no sign of local buckling of the steel tube. Local buckling of the steel tube could only be observed for the empty reference columns, and when it occurred it did so on at the compressive side at mid-height of the column.

The scatter between the test results within the same column type group was small. There was almost no difference in the load-deflection relationship when the load was applied to the concrete section

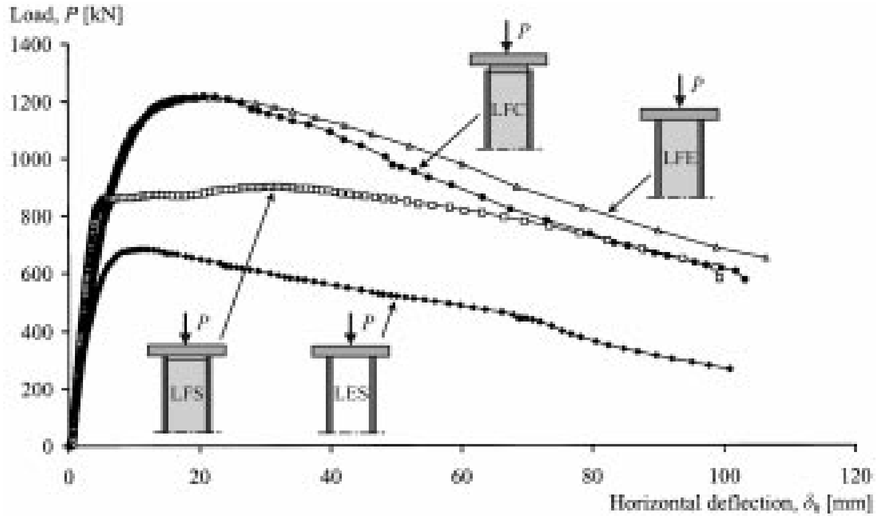

Fig. 4 Comparisons of load-deflection relationships for columns

Table 4 The measured maximum load-bearing resistance of the tested columns

Column type	Filled with concrete	Load application	Maximum load P_{max} (kN)	P_{max}/P_{ref} 1)
LES 1	no	steel	700	-
LES 2	no	steel	680	-
LFE 1	yes	entire	1210	1.75
LFE 2	yes	entire	1270	1.84
LFE 3	yes	entire	1220	1.77
LFC 1	yes	concrete	1220	1.77
LFC 2	yes	concrete	1200	1.74
LFC 3	yes	concrete	1250	1.81
LFS 1	yes	steel	860	1.25
LFS 2	yes	steel	820	1.19
LFS 3	yes	steel	850	1.23

1) P_{ref} = 690 kN, the mean value of the load resistance of the unfilled reference columns LES.

(LFC) or when it was applied to the entire section (LFE). However, when the load was applied to the steel section only (LFS) it could be observed that the load-bearing resistance was drastically reduced. In comparison with the reference column (LES), the load resistance for the LFS column was just approximately 20 percent higher; see Table 4. It seems that the load was not redistributed from the steel tube to the concrete core in a sufficient way and, consequently, the steel tube carried the major part of the applied load. After a horizontal deflection of approximately 20 mm, the load started to increase again for the LFS columns and approached the load levels of the LFE and LFC columns when the deflection was increased further. This was probably because the loading plate came in contact with the

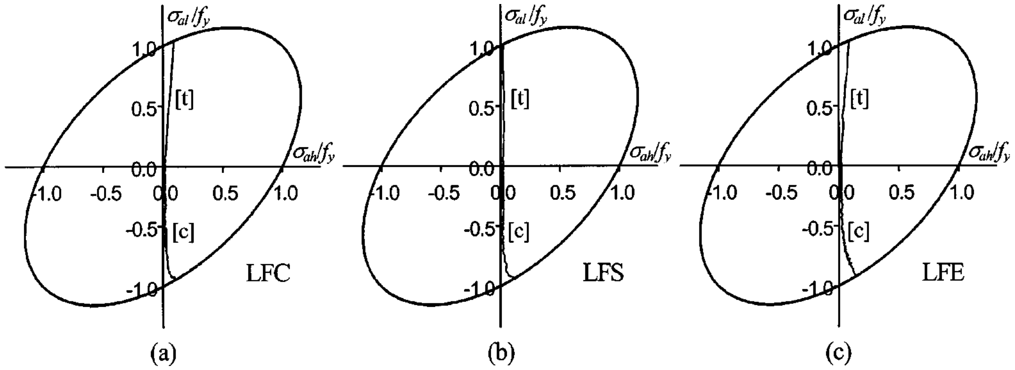

Fig. 5 The normalized steel stress path for the "compressive" [*c*] and "tensile" [*t*] sides of the columns

concrete core and it started to carry load. After the tests were finished it could be observed that the concrete core had slid in the steel tube and their surfaces were at the same level.

The measured maximum values of the load-bearing resistance for the tested columns, P_{max}, are tabulated in Table 4. Fig. 5 shows the normalized steel stress path up to the elastic limit, according to the von Mises yield criterion, for the "compressive" [*c*] and "tensile" [*t*] sides of the columns. The hoop steel stress, σ_{ah}, and the longitudinal steel stress, σ_{al}, are calculated from the measured strains, according to Hooke's Law with the assumption of plane state of stress; see Chen and Han (1988). The steel stress paths are similar for all the three different loading situations and no major hoop steel stresses are obtained.

3. Finite element analyses

3.1. Methodology

The aim of the finite element analyses was to extend the interpretation of the results and observations obtained in the tests, to gain a better understanding of the behavior of CFT columns. To facilitate study of composite columns, an established FE model should be able to simulate the columns in a realistic way; such phenomena as the bond between the concrete core and the steel tube, and the increase in concrete compressive strength due to confining effects, have to be taken into account. The nonlinear finite element analyses were performed with ABAQUS/Standard 5.7, HKS (1997).

3.2. Finite element models

3.2.1. General

The steel tube, the concrete core and the loading plates had to be separated from each other to simulate the bond between them: therefore they were defined as individual bodies. A three-dimensional finite element model based on solid elements was established and the interfaces between the steel tube, the concrete core and the loading plate were simulated by using surface-based interaction with a Coulomb friction model. To model the steel tube, 8-node solid elements with full integration were used, while for the concrete core and the loading plate, both 8-node and 6-node solid elements with reduced

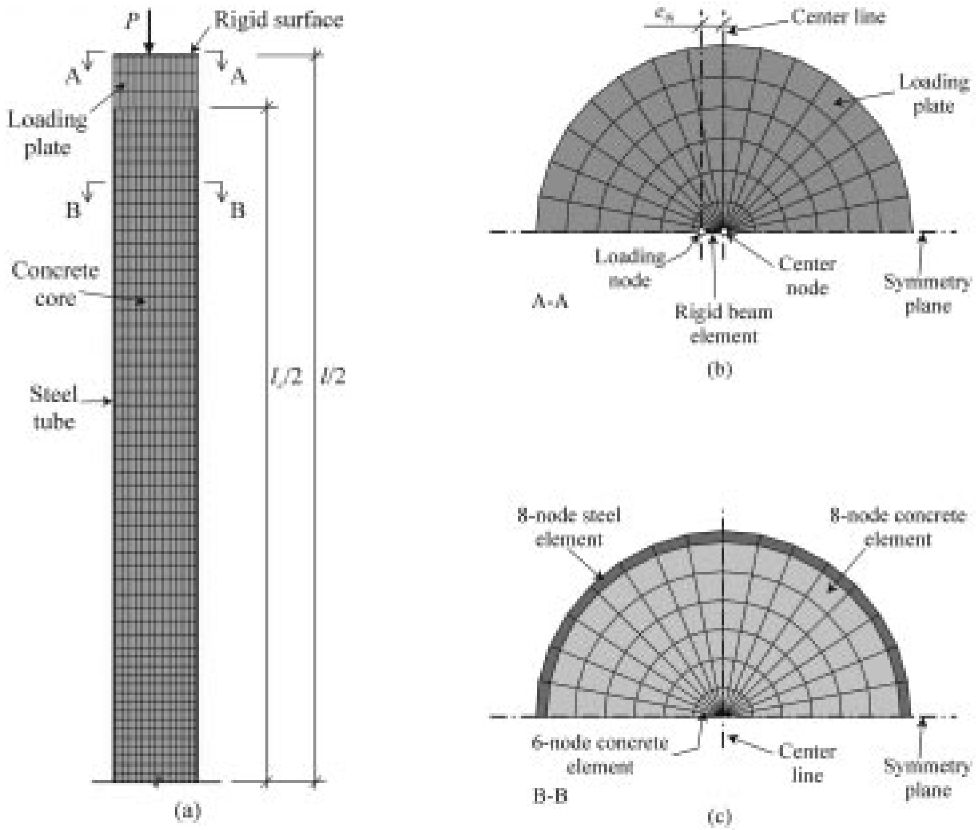

Fig. 6 The finite element mesh of the columns. (a) Half of the model, (b) the top of the loading plate and (c) section of the column

integration were used. In total the FE model of the slender columns consisted of 15251 elements. The symmetry plane perpendicular to the bending direction of the column was used to reduce the size of the FE model. Only half of the height of the column model is shown in Fig. 6. As in the tests, the column length is denoted l_c, and the buckling length of the column is denoted l. The curved bearing plate used in the tests was not modeled separately, but was included in the elements of the loading plate.

Since it was of interest to follow the post-peak behavior of the columns, the load was applied as an increased deformation at one node of the top loading plate. This loading node was positioned with an eccentricity from the centerline of the section and connected with the center node of the loading plate through a rigid beam element; see Fig. 6(b). The length of the rigid beam element thereby defined the size of the eccentricity. Further, the loading node was restrained from all horizontal translations. The corresponding node at the lower loading plate was restrained from all translations, horizontal as well as vertical. The center node was chosen as the reference node of the rigid surface, which was defined at the loading plate, to distribute the movements to the entire loading plate. As in the test series, the load was applied to the concrete section (a), to the steel section (b), or to the entire section (c); see Fig. 7. However, all the columns rested on the entire section at the bottom. Hence, the load arrangement in Fig. 7(c) was used at the bottom of the column in the FE model. The Newton-Raphson iteration method was

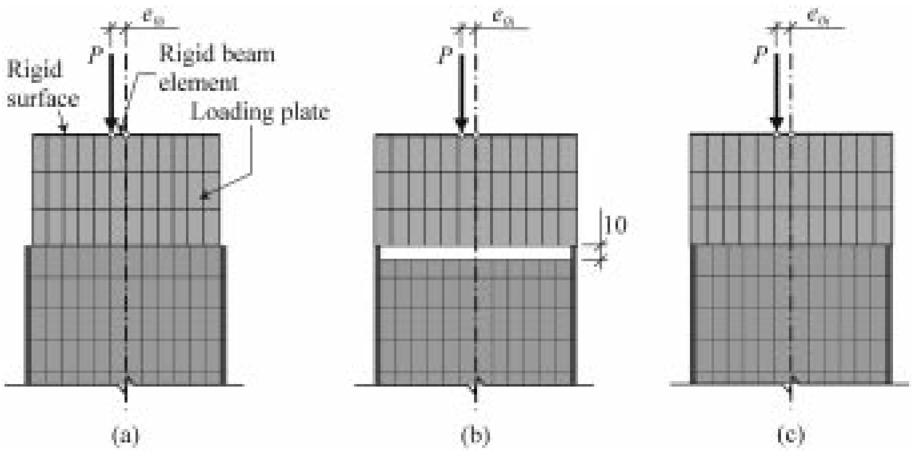

Fig. 7 The loading arrangement in the FE model. The load applied to the concrete section (a), to the steel section (b) and to the entire section (c)

used to find equilibrium within each load increment. Furthermore, the geometric nonlinear behavior was taken into account, i.e., the local buckling of the steel tube and the second-order effect were taken into consideration.

3.2.2. Modeling of the concrete

For plain concrete a special material option called "concrete" is provided in ABAQUS; see HKS (1997). The model uses a smeared crack approach, which means that it does not track individual "macro" cracks. Instead the localized deformation of each crack is smeared out over a characteristic length and the response in tension is described as a continuum in terms of stress-strain relations. In the FE model used in this study, the steel and concrete surfaces are allowed to move relative to each other; hence the characteristic length is taken as the element size in the vertical direction. A crack is assumed to occur when the stresses reach a failure surface called the "crack detection surface". The orientation of the crack is stored and remains fixed for the rest of the analysis. Additional cracks at the same point may form only orthogonal to this direction. Once cracking has appeared, the post-failure behavior of the concrete with open cracks is described by a damage elasticity model. A bilinear stress-crack opening relation, according to recommendations given in Gylltoft (1983), defines the tensile softening of the concrete, once the tensile strength has been exceeded. The fracture energy, G_F, together with the tensile strength, f_t, was used to calculate the ultimate crack opening, w_u, which in turn, together with the characteristic length, was used to determine the strain at zero stress. The concrete tensile strength, f_t, used in the analyses was determined from the compressive strength, $f_{c,cyl}$, proposed for high-strength concrete by the CEB Bulletin d'Information 228 (1995), as

$$f_t = 0.318(f_{c,cyl})^{0.6} \tag{1}$$

When the principal stress components are predominantly compressive, the response of the concrete is modeled by elastic-plastic theory. The elastic stress state is limited by a Drucker-Prager yield surface. Once yielding has occurred, an associated flow rule together with isotropic hardening is used. This model works well for uniaxial and biaxial compression; however, due to the formulation of the yield surface, for which the third stress invariant is not included, the response in triaxial compression is less accurate; see HKS (1997). The uniaxial stress-strain relations in compression, used in the analyses, were derived from standard cylinder tests with concrete from the same batch as the columns; see Table 2. In these tests the stress-strain relation could be registered only up to the maximum stress. The remaining part of the stress-strain relation was determined in accordance with the CEB Bulletin d'Information 228 (1995). However, it was shown that the material model is not sufficient to describe a triaxial stress state: hence, to capture the increase in ductility due to confinement in a reasonable way, the descending branch had to be assumed as a straight line with just a small inclination. Poisson's ratio in the elastic part was, according to recommendations in BBK 94, Boverket (1994), approximated as $\nu_c = 0.2$.

3.2.3. Modeling of the steel

An elastic-plastic model, with the von Mises yield criterion, associated flow rule and isotropic strain hardening, was used to describe the constitutive behavior of the steel; see HKS (1997). The complete stress-strain relation obtained from uniaxial tension tests on specimens taken from the steel tubes was used in the FE analyses. Poisson's ratio in the elastic part was set to $\nu_a = 0.3$.

3.2.4. Modeling of the interaction between steel and concrete

To simulate the bond between the steel tube and the concrete core, a surface-based interaction with a contact pressure-overclosure model in the normal direction, and a Coulomb friction model in the directions tangential to the surface, were used. In this way the surfaces could separate and slide relative to each other, as well as transmit contact pressure and shear stresses between the concrete core and the steel tube. In the basic form of the Coulomb friction model, two contacting surfaces can carry shear stresses across their interface up to a given magnitude before they start sliding relative to one another. The Coulomb friction model defines this critical shear stress, τ_{crit}, at which sliding between the surfaces starts. The critical shear stress is defined as a fraction of the contact pressure, p, between the surfaces ($\tau_{crit} = \mu p$), where μ is known as the coefficient of friction. According to Baltay and Gjelsvik (1990) and Boverket (1984), the coefficient of friction between concrete and steel has a value between 0.2 and 0.6. The contact pressure is given by the pressure-overclosure relationship. When the surfaces are in contact, any contact pressure can be transmitted between them; the contact pressure reduces to zero if the surfaces separate. Adhesion is an elastic brittle load transfer mechanism that is active mainly at the early stage of loading when the relative displacements are small. Its contribution to transfer load is therefore disregarded in this FE model.

3.3. Verification of FE model

To verify the FE model, a comparison of the results from tests and those from the FE analyses was made; see Fig. 8. The load-deflection relationships from the tests are represented by a shaded area, comprising the results of all columns of the same type. The coefficient of friction was set to 0.2 for all of the analyses in the verification of the FE model. It can be seen that the FE model captures the structural behavior in a satisfactory way. However, for the column with the load applied only to the steel section (LFS), the analysis stopped at approximately maximum load due to numerical problems. The reason for this has not yet been established. The maximum load resistances obtained in the FE analyses are equal to those obtained in the tests to within 6%, see Table 5. Nevertheless, the agreement between the strains obtained in the tests, measured by strain gages, and those obtained from FE analyses is good for all specimens. Further, a comparison of the deflected shape of the LFE column was

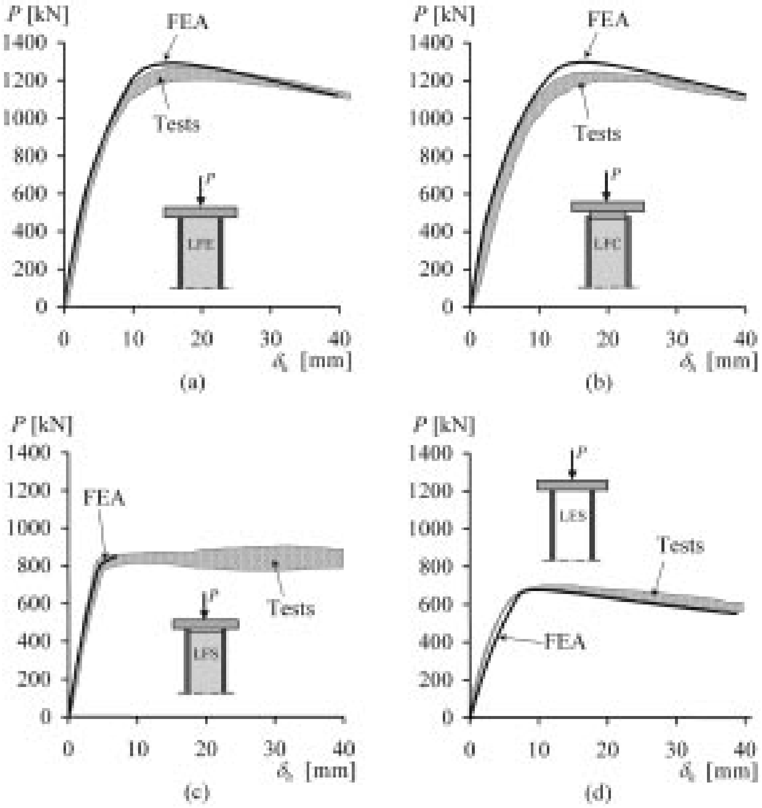

Fig. 8 Comparison of results of FE analyses and the tests for the columns. (a) Load applied to the entire section, (b) to the concrete section, (c) to the steel section and (d) empty steel tube as reference column

Table 5 Comparison of maximum load resistance obtained from the tests and the FE analyses

Column type	Load application	Maximum load P_{max} (kN) Test[1)]	FEA	Ratio FEA/Test
LES	steel	690	680	0.99
LFE	entire	1230	1290	1.05
LFC	concrete	1220	1290	1.06
LFS	steel	840	850	1.01

[1)]The mean values from the number of tests within the same column type group.

made; see Fig. 9. The deformed shape was plotted for the total buckling length, *l*, of the column. The rotation of the supports in the tests was assumed to be small and is neglected here, and the horizontal deflection is set to zero at the column ends. The compared deflected shapes were chosen to have approximately the same mid-height deflection in the analysis and in the tests. The table included in Fig. 9 shows the corresponding load of the deflected shape. Apart from the fact that the load is not exactly the same in the FE analysis and in test at a specific mid-height deflection, there is good agreement of the deflected shape of the column.

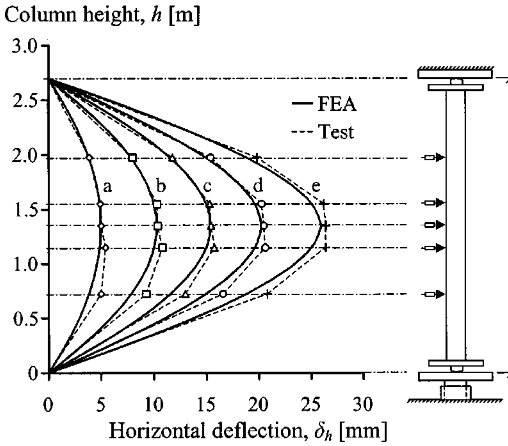

	P_{Test} [kN]	P_{FEA} [kN]
a	755	815
b	1110	1187
c	1191	1291
d	1216	1273
e	1200	1231

Fig. 9 Comparison of the deflected shape of the LFE column in the test and in the FE analysis

4. Results and discussion

4.1. General

It was observed in the results from the test series that the load resistance and also the structural behavior were influenced by how the load was applied to the CFT column. When the load was applied only to the concrete section (LFC) the load resistance was approximately the same as when the load was applied to the entire section (LFE). One question to be studied is why the load resistance is so drastically reduced when the load is applied only to the steel section (LFS). It appears that the applied load is not redistributed from the steel section to the concrete section in a sufficient way in this case. However, when the load is applied to the concrete section only, the load must be redistributed from the concrete to the steel in order to obtain the same load resistance as when the load is applied to the entire section. Furthermore, it is possible that the enhancement of concrete strength due to confinement influences the load resistance.

To better understand how the load is carried in the CFT columns under the various means of load application, the results obtained from the tests in combination with additional results from FE analyses have been studied. Fig. 10 shows how the axial force, N, in the columns is distributed between the concrete section and the steel section during the loading. The results are obtained from FE analyses. In order to compare the results, each curve was normalized with respect to the maximum load resistance, $P_{\max}$, of the column. The distribution was studied in the bottom section, where the columns were resting at both the steel and the concrete; i.e., the contributions by the steel tube and the concrete core to the total reaction force of the columns were examined. It can clearly be seen that there is almost no redistribution of the axial force from the steel section to the concrete core in the case with the load applied only to the steel section (LFS). Hence, the steel tube carries almost the entire load. However, the concrete core prevents the steel tube from buckling inwards and this seems to affect the stiffness as well as the load resistance.

In the tests it was observed that there was almost no difference in the load-deflection relationship when the load was applied to the concrete section (LFC), compared with when applied to the entire

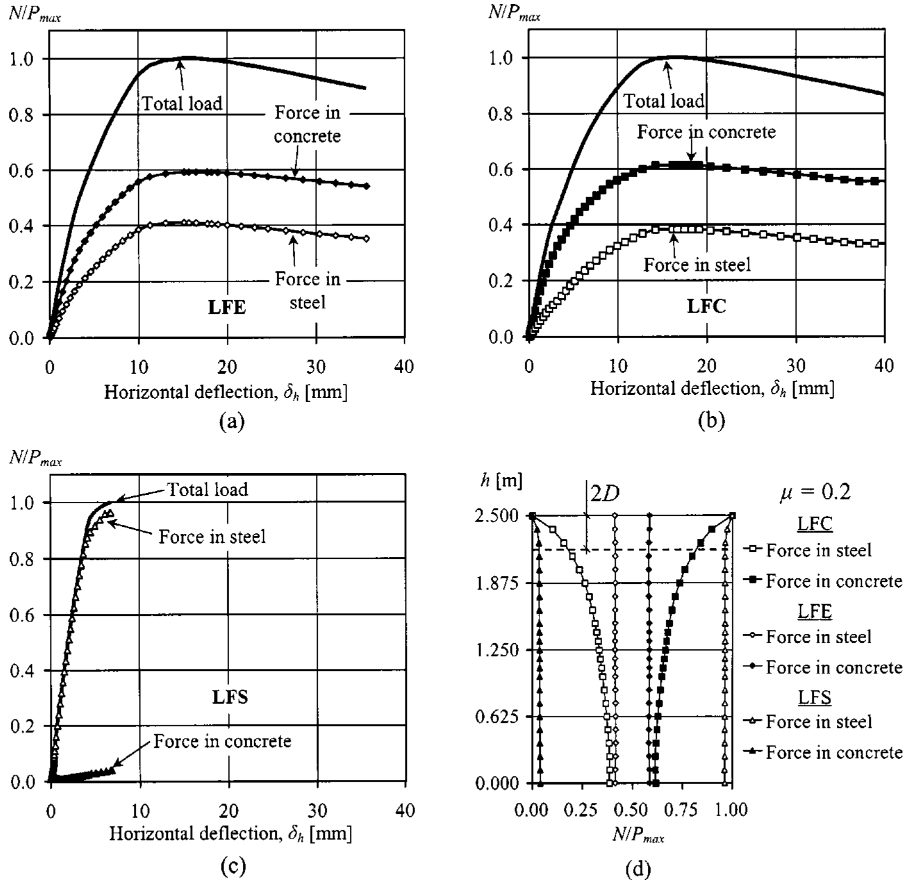

Fig. 10 Distribution of the axial force between the concrete section and the steel section versus deflection (a), (b) and (c) and over the height of the columns at maximum load (d), as obtained from FE analyses

section (LFE). In the FE analyses it can also be observed that the distribution of the axial force between the concrete core and steel tube at the bottom section is almost identical for both loading cases; see Fig. 10. Hence, for the LFC column the load was redistributed from the concrete section, under the loading plate at the top of the column, to the steel tube over the height of the column; see Fig. 10(d).

4.2. Influence of bond strength

It was shown that the axial force in the LFC and LFS columns was redistributed between the concrete core and the steel tube during the loading. Thus, when the load is applied only to the steel section or only to the concrete section, the axial force in the column must be transferred over the contact surface between the concrete core and the steel tube. Therefore, it is reasonable to think that the bond strength between the concrete core and the steel tube influences how the axial force is distributed in a section and, further, influences the structural behavior and the load resistance of the CFT column. Because adhesion is active mainly at the early stage of loading, it is disregarded in the FE analyses and the shear stresses between the concrete and the steel are assumed to be only a result of friction. Friction develops between the concrete core and the steel tube due to normal contact pressure, for instance caused by lateral expansion of the concrete core when subjected to compressive loading. The magnitude of the friction force developed in CFT columns depends on the rigidity of the tube walls against pressure perpendicular to their plane.

To study the influence of the bond strength for the three types of loading conditions studied, additional analyses with coefficient of friction, μ, set to 0.0, 0.6 or 1.0 between the concrete core and the steel tube were performed. Fig. 10(d) shows how the axial force, N, in the column was distributed between the concrete core and the steel tube at different heights of the columns, when the maximum load capacities of the columns were reached. Each curve has been normalized with respect to the total applied load, P. In this case the coefficient of friction was 0.2. When the load was applied to the entire section (LFE), the contributions by the concrete core and steel tube to the total axial force were constant along the height of the column, and were not affected by an increased coefficient of friction. Further, the bond strength had no influence on the structural behavior of the column. In contrast, when the load was applied to the concrete section (LFC), the axial force was gradually transferred from the concrete to the steel from the top to the bottom of the column. It can be seen that the distribution between the concrete core and the steel tube in this case approaches the same distribution at the bottom of the column, as when the load was applied to the entire section. When a higher value of the friction coefficient was used, the transmission length decreased, compared with when a lower value was used; i.e., the axial force was redistributed faster between the concrete section and the steel section; see Fig. 11(b).

It should be noted that although the distribution of the axial force, between the concrete section and the steel section, changed when the coefficient of friction was set to 0.2, 0.6 or 1.0, the structural behavior and the maximum load resistance were almost identical in all three cases; see Fig. 11(a). However, when the coefficient of friction was set to 0.0 almost no axial force was redistributed from the concrete core to the steel tube, and as a consequence a drastic change in the load-deflection relationship can be observed; see Fig. 11. When the load was applied to the steel section (LFS), it can be seen, in Fig. 10(d), that the steel tube carried almost the whole load through the column and a higher coefficient of friction gave just a small increase in the load resistance.

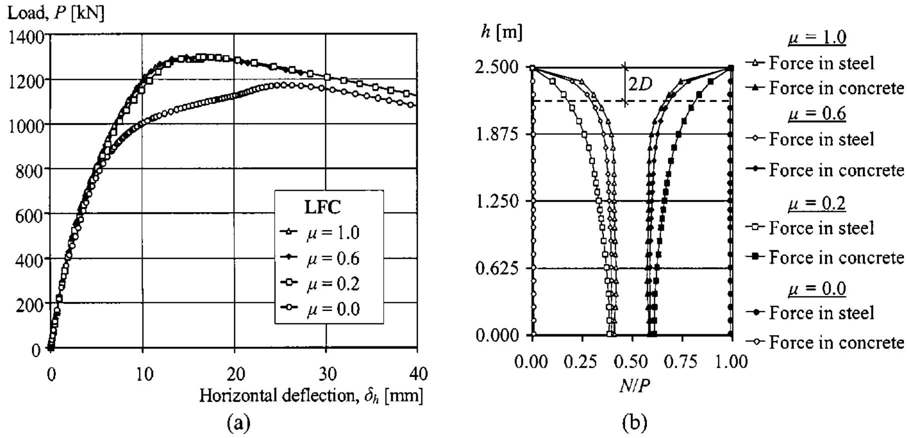

Fig. 11 Influence of bond strength on the behavior of columns loaded on the concrete section: (a) load-deflection relations and (b) distribution of axial force over the height of the columns

According to Eurocode 4 (1992), the transmission length of the shear force should not be assumed to exceed twice the transverse dimension, here twice the diameter of the column (2*D*). It can be noted that this is fulfilled only when the load is applied to the entire section, see Figs. 10 and 11. Provided that the concrete and the steel sections are loaded simultaneously for the LFE column, this study has indicated that the bond strength seems to have little or no influence on the structural behavior, the load resistance, or the distribution of the axial forces. Experimental studies by Grauers (1993) and Kilpatrick and Rangan (1999b) have also indicated this. Hence, the composite action can be taken into account as long as the load is applied at the entire section of the column. However, for columns with the load applied to the concrete section or the steel section only, it seems necessary to provide the top region of the steel tube with mechanical shear connectors at the inside to ensure full composite action. According to Roeder *et al.* (1999) far less bond stress demand is required in regions of beam-to-column connections, where elements penetrate the concrete core and cause a blocking action, than in direct steel-to-steel connections. This confirms the findings in our paper, since the load introduction to the LFE and LFS columns can be referred to the former the and latter case, respectively.

4.3. Influence of confinement

It was observed in this study that the concrete core contributed to carrying the total axial force, when the load was applied to the entire section or to the concrete section only. In the critical section at mid-height of the column, the concrete core carried approximately 60% and 65% of the total axial force for the LFE column and the LFC column, respectively; see Fig. 10. It is of interest to see if any part of the load carried by the concrete core is an effect of increased concrete compressive strength due to the triaxial compressive stress state caused by confinement of the concrete core. In a CFT column, compressive confining stresses on the concrete core are induced by passive confinement provided by the steel tube. A circular steel tube has a high stiffness against inner pressure perpendicular to the tube wall, and therefore effective circumferential steel hoop tension can develop to provide lateral confining pressure to the concrete core. In the case of passive confinement, the confining pressure is not constant as is the case for active confinement, and also depends on the lateral deformation of the concrete core under axial load and the stress-strain relationship of the confining steel. Nevertheless, it has been found that the concrete behavior was similar irrespective of whether the confining pressure is active or passive; see Attard *et al.* (1996). However, for these slender columns no significant effect of increased compressive strength in the concrete core due to confinement was observed in the critical section of the column at the maximum load resistance; see Fig. 12. The higher contribution to the total axial force by the concrete core for the LFC column results in an increased zone, where the maximum concrete strength has been reached, compared with the LFE column. It was also shown in Fig. 5 that the circumferential steel stresses were low for both the LFC and LFE columns, which indicates a low confining pressure on the concrete core and consequently less increase of concrete strength.

These observations indicate that the slender CFT columns in this study did not exhibit the beneficial effects of composite behavior by means of increased concrete strength due to confinement of the concrete core. This is most likely caused by an increasing strain gradient of the cross-section with increasing flexure. This inference is also generally supported in previous research by Furlong (1967), Knowles and Park (1969), Neogi *et al.* (1969) and Kilpatrick and Rangan (1999b). The increase in concrete strength due to confinement of the concrete core by the steel tube has been found to be valid only for columns with a slenderness ratio below a certain limiting value. For instance, according to Eurocode 4 (1992) the effect of confinement is considered when the non-dimensional slenderness ratio

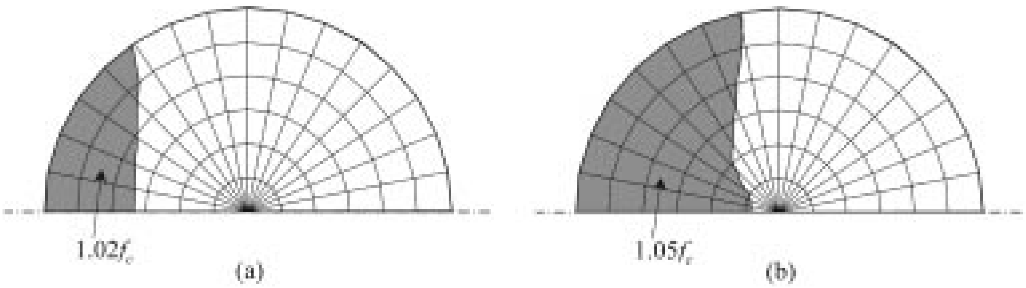

Fig. 12 The part of the compressive zone in which the compressive stresses are greater than the uniaxial compressive strength of the concrete. The load was applied to (a) the entire section or to (b) the concrete section

$\bar{\lambda}$ is less then 0.5. The slenderness ratio is defined as

$$\bar{\lambda} = \sqrt{\frac{N_{pl,R}}{N_{cr}}} \tag{2}$$

where $N_{pl.R}$ is the plastic resistance to compression of the composite cross section and N_{cr} is the elastic critical load of the column. This is valid under the condition that the eccentricity of the normal force calculated by first-order theory, at the same time, does not exceed the value $D/10$, in which D is the external diameter of the column. For the columns in this study the slenderness ratio is approximately 0.86, and hence above the limiting value for which the confinement effect is to be taken into consideration. However, after the maximum concrete compressive strength has been reached, the steel tube prevents the concrete from spalling and the concrete core continues to carry high stresses with increased strains, thereby influencing the ductility of the CFT column; see Fig. 10.

5. Conclusions

The results obtained from tests and FE analyses on the circular steel-concrete composite columns presented in this paper allow the following conclusions to be drawn. For all the columns the maximum load capacity was determined by global buckling with no sign of local buckling of the steel tube at the critical cross-section. Local buckling of the steel tube could be observed only for the empty reference columns in the later part of the loading. The columns in this study did not exhibit the beneficial effects of composite behavior by means of increased concrete strength due to confinement of the concrete core. However, the steel tube prevents the concrete from spalling and the concrete core continues to carry high stresses with increased strains and thereby influences the ductility.

When the load was applied to the entire section, the contribution by the concrete core and steel tube to the total axial force was constant along the height of the column, and was not affected by the bond strength. Further, the bond strength had no influence on the structural behavior of the column. However, when the load was applied only to the concrete section, the axial force was gradually transferred from the concrete to the steel, and the distribution as well as the structural behavior were affected by changed bond strength. When the load was applied only to the steel section, the natural bond strength was not sufficient to redistribute force to the concrete core. Finally, to get full composite action it does not seem to be enough to rely on the natural bond strength when connection details are attached only to the steel tube or concrete core. Instead, the connection design should force the entire section to undergo the same deformations.

Acknowledgements

The first author conducted the work presented in this paper as part of his PhD studies at Chalmers University of Technology under the supervision of the second author. The authors wish to express their gratitude to the Swedish Council for Building Research (BFR), the Development Fund of the Swedish Construction Industry (SBUF) and the construction company NCC AB, for financially supporting this project.

References

Attard, M.M. and Setung, S. (1996), “Stress-strain relationship of confined and unconfined concrete”, *ACI Materials Journal*, Sept.-Oct. 1996, Title no. 93-M49, 432-442.

Baltay, P. and Gjelsvik, A. (1990), “Coefficient of friction for steel on concrete at high normal stress”, *J. Materials in Civil Eng.*, **2**(1), February 1990, 46-49.

Boverket (1994), *Boverkets Handbok för Betongkonstruktioner BBK 94, Band 1, Konstruktion* (Boverket´s Handbook for Concrete Structures, BBK 94, Vol. **1**, Design. In Swedish). Boverket, Byggavdelningen, Karlskrona, Sweden, 185 pp.

BST Byggstandardisering (1991), *Betongprovning med Svensk Standard BST Handbok 12, Utgåva 6* (Swedish Standards for Concrete Testing, BST Handbook 12, Sixth edition. In Swedish), SIS Standardiseringskommissionen i Sverige och Svensk Byggtjänst, Stockholm, 286 pp.

CEB Bulletin d'Information 228. (1995), *High Performance Concrete, Recommended Extensions to the Model Code 90*, Research Needs. Lausanne, Switzerland, July 1995.

Chen, W.J. and Han, D.J. (1988), *Plasticity for Structural Engineers*, Springer-Verlag New York Inc., USA, 1988, 606 pp.

European Prestandard, Eurocode 4 (1992), “Design of composite steel and concrete structures, Part 1-1: General rules and rules for buildings”, Ref. No. 1994-1-1:1992, October 1992, 180.

Furlong, R.W. (1967), “Strength of steel-encased concrete beam columns”, *J. Struct. Div.*, Proc. ASCE, **93**(ST5), October 1967, 113-124.

Grauers, M. (1993), *Composite Columns of Hollow Steel Sections Filled with High Strength Concrete*. Publication 93:2, Ph.D. dissertation, Chalmers University of Technology, Division of Concrete Structures, Göteborg, Sweden, June 1993, 236 pp.

Gylltoft, K. (1983), *Fracture Mechanics Models for Fatigue in Concrete Structures*. 1983:25D, Luleå University of Technology, Division of Structural Engineering, Luleå, Sweden, 210 pp.

Hajjar, J.F., Schiller, P.H. and Molodan, A. (1998), “A distributed plasticity model for concrete-filled steel tube beam-columns with interlayer slip”, *Eng. Struct.*, **20**(8), Aug. 1998, 663-676.

HKS (1997), *ABAQUS/Standard User's Manual, version 5.7*, Hibbit, Karlsson & Sorensen, Inc., Pawtucket.

Johansson, M. (2000), “Structural behaviour of circular steel-concrete composite columns: non-linear finite element analyses and experiments”, Licentiate thesis, Chalmers University of Technology, Div. of Concrete Struct., Göteborg, Sweden.

Kilpatrick, A.E. and Rangan, B.V. (1999a), “Tests on high-strength concrete-filled steel tubular columns”, *ACI Structural Journal*, March-April 1999, Title no. 96-S29, 268-274.

Kilpatrick, A.E. and Rangan, B.V. (1999b), “Influence of interfacial shear transfer on behavior of concrete-filled steel tubular columns", *ACI Structural Journal*, July-Aug. 1999, Title no. 96-S72, 642-648.

Knowles, R.B. and Park, R. (1969), "Strength of concrete filled steel tubular columns", *J. Struct. Div.*, ASCE, **95**(ST12), Dec. 1969, 2565-2587.

Neogi, P.K., Sen, H.K. and Chapman, J.C. (1969), "Concrete-filled tubular steel columns under eccentric loading", *The Structural Journal*, **47**(5), May 1969, 187-195.

RILEM 50-FMC Committee (1985), "Determination of the fracture energy of mortar and concrete by means of three-point bend tests on notched beams", *Material and Structures*, **18**(106), 285-290.

Roeder, C.W., Cameron, B. and Brown, C.B. (1999), "Composite action in concrete filled tubes", *J. Struct. Eng.*, **125**(5), May 1999, 477-484.

Shams, M. and Saadeghvaziri, M.A. (1997), "State of the art of concrete-filled steel tubular columns", *ACI Structural Journal*, Sept.-Oct. 1997, Title no. 94-S51, 558-571.

SS 11 21 19: *Metalliska Material Dragprovstavar av Rör Rörstrimlor Typ J* (Metallic materials Tensile test pieces from tubes Test pieces type J. In Swedish). SIS Standardiseringskommissionen i Sverige, Sweden, 1986.

CC